An investigation of the dye palette in Chinese silk embroidery from Dunhuang (Tang dynasty)

Diego Tamburini, Caroline R. Cartwright, Monique Pullan & Hannah Vickers

Archaeological and Anthropological Sciences

ISSN 1866-9557
Volume 11
Number 4

Archaeol Anthropol Sci (2019)
11:1221-1239
DOI 10.1007/s12520-017-0592-4

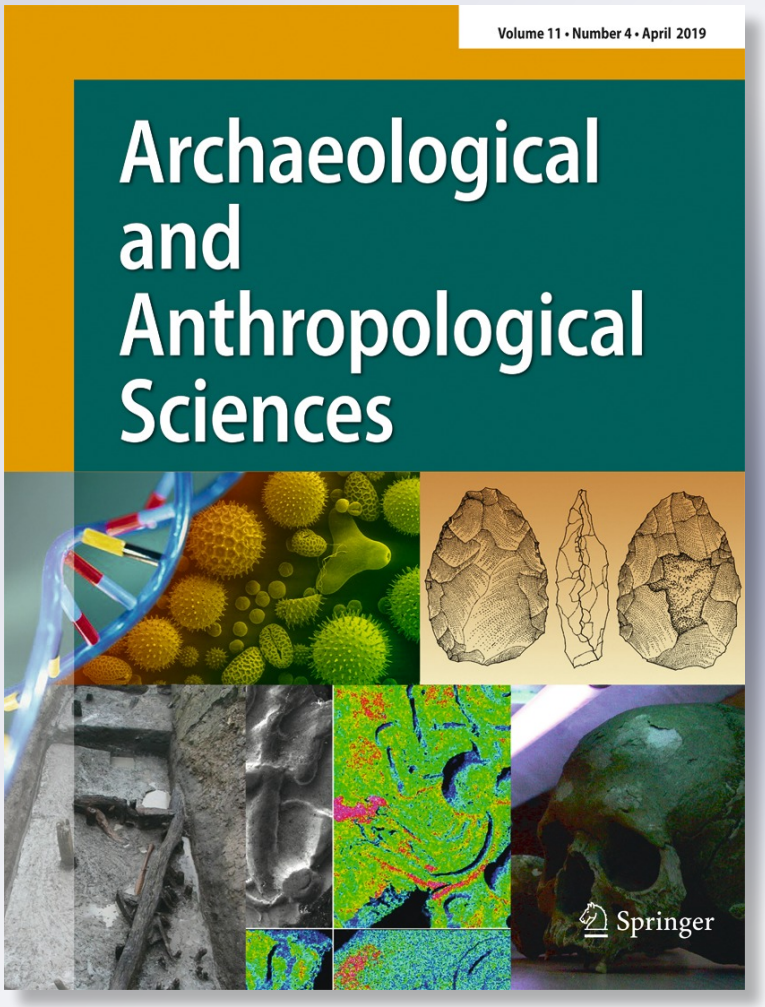

Springer

Archaeological and Anthropological Sciences (2019) 11:1221–1239
https://doi.org/10.1007/s12520-017-0592-4

ORIGINAL PAPER

An investigation of the dye palette in Chinese silk embroidery from Dunhuang (Tang dynasty)

Diego Tamburini[1] · Caroline R. Cartwright[1] · Monique Pullan[2] · Hannah Vickers[2]

Received: 2 November 2017 / Accepted: 25 December 2017 / Published online: 30 January 2018

Abstract

'Sakyamuni preaching on Vulture Peak' is one of the largest known Chinese silk embroideries thought to date to the eighth century, under the Tang dynasty (618–907). It was found at the cave temple site of Qian Fo Dong, near Dunhuang, one of the most famous archaeological sites in China, and is now in the British Museum (BM). Scanning electron microscopy (SEM) was used to investigate the state of degradation of the original and restoration fibres, which appeared very brittle in many areas. Energy dispersive X-ray (EDX) spectrometry was undertaken to give an indication of the mordants. Although the results were difficult to interpret due to elemental contamination, some indications were obtained regarding aluminium and iron mordants on the silk embroidery. Selected dyed threads were sampled and analysed using high pressure liquid chromatography coupled with mass spectrometry (HPLC-MS). The samples were representative of the entire dye palette used. In some of the areas that are now demonstrated to be extremely faded, safflower (*Carthamus tinctorius*) was identified. More than one source of indigotin was probably used for the blues, and the greens were obtained by mixing these with at least two sources of yellow dyes: a berberine- and a luteolin-based dye. Browns were tannin-based. Two sources of reds were also present: a plant of the Rubiaceae family and a currently unknown red source. The presence of shikonin, probably from gromwell (*Lithospermum erythrorhizon*), was revealed in a purple stripe in mixture with sappan wood *Caesalpinia sappan* (*Biancaea sappan*) to obtain a particular hue. Other molecular components were often present with the main dyes and tandem mass spectra were acquired in an attempt to elucidate their structures and discuss the possible reasons for their presence. This work represents an important addition to the current knowledge about Chinese dyes and available mass spectral data for the identification of dye sources in archaeological textiles from the Silk Road.

Keywords Chinese embroidery · Silk road textiles · Dye analysis · Fibre degradation · SEM-EDX · HPLC-MS

Introduction

The 'Sakyamuni preaching on Vulture Peak' embroidery, referred to as 'Vulture Peak', was found at the cave temple site of Qian Fo Dong, near Dunhuang, on the edge of the Gobi desert in western China. Historically, this was an important hub of cultural, religious and commercial exchange on the network of trade routes known as the Silk Road. The caves were in active use as Buddhist temples from the fourth century until they were largely abandoned in the fourteenth century and represent one of the most famous archaeological sites in China (Cave Temples of Dunhuang: Buddhist Art on China's Silk Road 2016; Fan and Yongzeng 2007; Stein 1912).

The 'Vulture Peak' embroidery was recovered in 1900 from Cave 17, known as the Hidden Library Cave, by the abbot of the temples, Wang Yuanlu. The cave had been sealed with plaster and, when opened, was found to contain thousands of scrolls, manuscripts and textiles. Dating of the most recent manuscripts suggests that the cave had been sealed in the eleventh century. Therefore, the contents had remained undisturbed for at least 800 years. The conditions of the cave proved ideal for preserving the ancient textiles stored inside,

Electronic supplementary material The online version of this article. (https://doi.org/10.1007/s12520-017-0592-4) contains supplementary material, which is available to authorized users.

✉ Diego Tamburini
DTamburini@britishmuseum.org

[1] Department of Scientific Research, The British Museum, Great Russell Street, London WC1B 3DG, UK

[2] Department of Conservation, The British Museum, Great Russell Street, London WC1B 3DG, UK

including the 'Vulture Peak' embroidery, thought to date to the eighth century or earlier. The textile was probably used as a devotional panel in the cave temples over a substantial period of time, and may have been made at the site. The embroidery is worked in silk floss thread in many different colours, which are still vibrant today despite evidence of fading (Fig. 1).

The panel is a rare surviving example of a large well-preserved eighth century embroidery, and therefore provides an extremely valuable insight into ancient Chinese textile production, dyeing and trade (Cave Temples of Dunhuang: Buddhist Art on China's Silk Road 2016; Fan and Yongzeng 2007; Stein 1912). For this reason, the main aim of this work was to characterise the dyes used to obtain such a broad palette of colours, which are extremely rarely found on a single textile of this age, as well as to acquire information on the mordants and on fibre degradation.

Several publications have described conservation and scientific work undertaken in Dunhuang and related archaeological sites (Cave Temples of Dunhuang: Buddhist Art on China's Silk Road 2016; Cave Temples of Mogao at Dunhuang: Art and History on the Silk Road 2015; Conservation of Ancient Sites on the Silk Road 1997; Conservation of Ancient Sites on the Silk Road 2010; The Conservation of Cave 85 at the Mogao Grottoes, Dunhuang 2013). These mainly focused on the study of the materials used to produce the outstanding mural paintings in the caves in order to preserve them. Few scientific studies have covered the textiles, which remain relatively poorly investigated. However, the relevant Dunhuang textiles present in UK collections (British Museum, British Library and Victoria and Albert Museum) have been beautifully catalogued and described (Feng 2007).

Nevertheless, information on Asian colourants is relatively limited in Western literature. Combining information from various sources, including ancient texts, around 40 plants are listed among the most common raw materials for dyeing blue, red, yellow and brown in ancient China (De Luca et al. 2016; Grzywacz et al. 2004; Han et al. 2017; Laursen et al. 2015). However, investigations on ancient Chinese textiles from different periods often report the detection of unknown dyes, showing the need for further research in this field and highlighting the lack of reference material (Jolly et al. 2017; Karpova et al. 2016; Zhang et al. 2007; Zhang et al. 2008).

Non-destructive surface techniques, such as TOF-SIMS, SERS, FTIR, fluorescence and UV-Vis reflectance spectroscopy have been applied to the identification of a limited number of Asian colourants (De Luca et al. 2016; Lee et al. 2013; Nakamura et al. 2009; Sasaki and Sasaki 2017), but high pressure liquid chromatography (HPLC) coupled with UV/Vis detectors (PDA) (De Luca et al. 2016; Gibbs et al. 1997; Jolly et al. 2017; Karpova et al. 2016; Mouri and Laursen 2011; Sasaki and Sasaki 2013; Zhang et al. 2007; Zhang et al. 2008; Zhang et al. 2017) and/or mass spectrometry (HPLC-MS) (Degano et al. 2009; Pauk et al. 2014; Rosenberg 2008) is the state of the art technique to identify dyes in ancient textiles. HPLC-MS has been seldom used with application to Chinese dyes (Han et al. 2017; Laursen et al.

Fig. 1 'Sakyamuni preaching on Vulture Peak' (dimensions 167 × 249 cm), showing the sampling positions. D and F refer to samples taken for dye analysis and fibre characterisation, respectively. © The Trustees of the British Museum

2015; Zhang et al. 2017); therefore, MS data for identification are not easily available. The extraction of the dye molecules from the fibres is also a crucial step in this type of analysis. Today, scholars and researchers agree that mild extraction procedures, avoiding strong acids such as HCl, have to be adopted in the first instance, as these enable informative glycosidic bonds and sensitive molecules to be preserved (Degano and La Nasa 2016; Gulmini et al. 2016; Lombardi et al. 2016; Manhita et al. 2011; Mouri and Laursen 2012; Pauk et al. 2014).

This work provides a detailed analysis of the dye palette of the 'Vulture Peak' embroidery by HPLC-MS, thus providing new insights into the use of organic colourants in Tang dynasty China and increasing the database of MS/MS spectra of molecular markers useful for the identification of Asian dyeing plants. The study is complemented by the analysis of mordants by SEM-EDX and, for the purposes of informing the conservation, the assessment of the degradation state of fibres by SEM, as well as by the description of the conservation work undertaken.

Materials and methods

Sakyamuni preaching on Vulture Peak

The textile is a large Buddhist embroidered panel depicting the standing figure of Buddha Sakyamuni preaching on Vulture Peak, attended by bodhisattvas and disciples on either side (Fig. 1). It also depicts *apsaras* flying overhead, attendant lions and small donor figures on either side of a dedicatory panel below. The entire panel measures approximately 167 × 249 cm, and is thought to date to the eighth century (Tang dynasty, 618–907 AD). The dating is based on stylistic evidence, as no radiocarbon dating was performed. However, recent studies of some writings present on the object revealed a reference to the Mogao Grottoes that was in use only until the end of the seventh century. Chronologically this would place the panel more towards the beginning of the Tang dynasty, but further studies are needed to provide certain attribution. The design comprises extensive embroidery closely worked in silk floss of numerous colours, stitched through a silk ground and hemp backing. It has two large areas of loss already present when the embroidery was found. Original patch repairs and evidence of different stages of stitching suggest that the embroidery had been repaired during its period of use before being sealed in the Hidden Library Cave of Qian Fo Dong in the eleventh century.

The embroidery was brought to the British Museum in 1908 by Sir Aurel Stein after his second expedition to Qian Fo Dong (Stein 1912). The embroidery was restored at the Royal School of Needlework by Miss E. A. Winter, probably in 1912. This restoration treatment involved stitching the panel to a linen backing fabric, which was then attached to a large wooden crossbar stretcher.

Conservation work was carried out in 2017 in order to stabilise the embroidery for storage and loan. The earlier restoration had now begun to fail, leaving the embroidery at risk of further damage. Therefore, the decision was made to remove the previous restoration and stretcher and replace it with a new conservation treatment and mounting system. The project provided a unique chance to sample and analyse the textile, particularly when the removal of the previous restoration backing permitted brief access to the reverse of the original panel.

Visual examinations

The conservation team carried out a visual examination of the panel under UV light, using a UV Hand Luminaires (CLE Design Ltd.) in order to obtain preliminary information on the fluorescence of the dyes through observation and mapping of the threads (Fig. 2). This preliminary examination revealed some differences between dyed threads that had

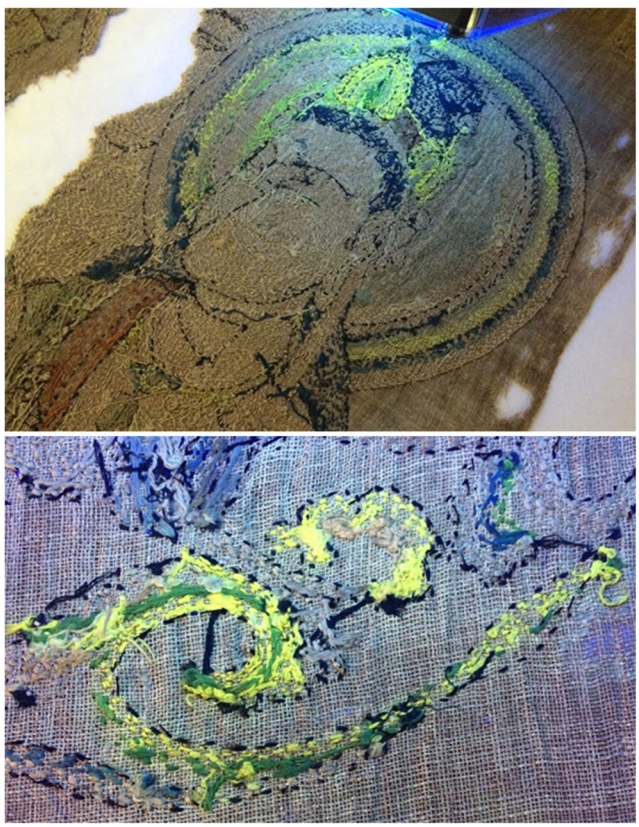

Fig. 2 Details of examination under UV light performed on the backing of the embroidery. A strong yellow fluorescence (both top and bottom) was observed for some yellow threads but not for others. An orange fluorescence (bottom) was observed on other areas. These types of fluorescence are consistent with berberine-type and safflower dyes, respectively. Images: H. Vickers and M. Pullan © The Trustees of the British Museum

appeared the same under normal light and also suggested the presence of dyes no longer visible to the naked eye due to fading. This was also important to guide the sampling and reconstruct the distribution of certain colours on the original panel.

Sampling

Samples (ca. 3 mm) were taken with the aim to include the whole palette of dyes and all the types of fibres present. The mass of the samples ranged from ca. 50 to ca. 150 μg.

Fifteeen tiny samples ('F' suffix) were taken mainly from the edges of the front of the embroidery for fibre characterisation and evaluation of their state of degradation. Twenty-five samples ('D' suffix) were taken with particular attention to dye and mordant analyses.

Eighteen 'D' samples were taken from the front of the panel. This sampling allowed access to a limited number of colours, such as blues, greens, yellows, browns and one of the two reds. When the textile was turned to replace its backing, the rear of the embroidery became accessible, as did all the remaining colours. Seven samples were then taken from the back, including the red and the purple from the robe of the central figure and the pink from the halo. The pink colour was not clearly visible from the front of the panel, as it almost completely faded. However, it appeared vibrant in some areas of the back, particularly one of the stripes in the halo of the Buddha and other details from the garments and the flower (Fig. S1, Supplementary material). Some of these samples actually represented the knots constituting the end of the embroidery threads, which had become detached naturally from the textile.

The sampling locations for all the samples are shown in Fig. 1. A description and some optical microscopy images of the samples are present in Table 1.

SEM-EDX

Scanning electron microscopy (SEM) was used to investigate all the samples from the 'F' series for fibre characterisation and assessment of their state of degradation in order to answer specific conservation questions.

Each sample was placed uncoated on an adhesive carbon disc mounted onto an aluminium SEM stub; no other sample preparation was undertaken. Examination of the samples and comparative reference specimens was undertaken in the VP SEM (Hitachi S-3700N) using the backscatter electron (BSE) detector mostly at 16 kV but sometimes also at 12 kV, depending on the sample. Magnifications ranged from ×20 to ×750. The preferred working distance was *c.*12 mm, but extended from 7 to 19 mm (as required). The SEM chamber was only partially evacuated (mostly 40 Pa, sometimes 30 Pa). With the BSE detector, 3D mode (rather than compositional) was preferentially selected to maximise the opportunity to reveal diagnostic features for identification as well as traces of degradation, wear, abrasion or particulate matter (see Fig. 4a).

The EDX detector was used to analyse some of the samples from the 'D' series representative of the majority of the colours. In particular, samples 6D (blue), 17D (yellow), 18D (brown), 19D (red), 20D (pink), 22D (green), 23D (red) and 25D (purple) were analysed. In the case of these samples, single fibres were isolated from the bigger samples shown in Table 1 and placed on an SEM stub. The instrumental parameters used for observation were the same as described above, except for the working distance, which was kept at 10 mm, which is optimal for EDX analysis. EDX spectra were acquired for 1 min in the energy range 0–20 eV and with number of channels 2048. AZtecEnergy analysis software (Oxford Instruments) was used to process the data.

HPLC-DAD-ESI-Q-ToF

A mild extraction procedure was adopted to extract the dyes: the samples were put in 2 mL vials, admixed with 200 μL DMSO and heated at 80 °C for 10 min. After centrifugation, the supernatant was transferred into another vial. The residue was admixed with 200 μL of methanol/acetone/water/0.5 M oxalic acid 30:30:40:1 (*v*/*v*/*v*/*v*) and heated at 80 °C for 15 min. The solution was evaporated under N_2 and reconstituted using 200 μL of MeOH/H_2O 1:1 (*v*/*v*). The DMSO extract was combined with the oxalic acid extract and the solution was centrifuged for 10 min. The supernatant was transferred to a fresh 250 μL insert and 5–10 μL of the solution were injected into the HPLC system. The extraction procedure was optimised in the framework of the CHARISMA project (2009–2014) funded by the European Union FP 7 Research Infrastructures programme (CHARISMA Grant Agreement no. 228330) and has proven its suitability for the analysis of organic colourants in both dyes (Han et al. 2017) and pigments formulations (Dyer and Tamburini 2017; Tamburini et al. 2018). The successful use of oxalic acid is also reported in slightly different methods (Mouri and Laursen 2012; Santos et al. 2015).

Analyses were carried out using a 1260 Infinity HPLC (Agilent Technologies), coupled to a Quadrupole-Time of Flight tandem mass spectrometer 6530 Infinity Q-ToF detector (Agilent Technologies) by a Jet Stream ESI interface (Agilent Technologies). The HPLC conditions were Zorbax Extend-C18 column (2.1 mm × 50 mm, 1.8-μm particle size); 0.4 mL/min flow rate; 5 μL injection volume for MS experiments and 10 μL for MSMS experiments; 40 °C column temperature. Separation was achieved using a gradient of water with 0.1% formic acid (eluent A) and acetonitrile with 0.1% formic acid (eluent B). The elution gradient was programmed as follows: initial conditions

Table 1 List and description of the samples analysed, including some optical microscopy images obtained at ×80 magnification

Sample	Colour	Description	Image
Samples for fibre analysis (F series)			
1F		Original hemp (layer 1)	
2F		Ground silk weft	
3F		Original hemp (layer 2)	
4F		Original hemp (patch)	
5F		Ground silk warp	
6F	Light blue	Floss silk	
7F	Orange	1900s restoration thread	
8F	Beige	1900s restoration silk	
9F	Dark blue	Silk embroidery thread	
10F		Edge of 1900s restoration stitch	
11F	Dark brown	Original outline thread	
12F		Original fluffy thread at bottom	
13F	Cream	Original silk	
14F	Cream	Original silk	
15F		Linen 1900s restoration backing	
Samples for dye/mordant analysis (D series)			
1D	Pale yellow	Forehead of partially missing figure on left hand side	Not available
2D	Pale yellow	Lightest coloured stripe of halo of partially missing figure on left hand side	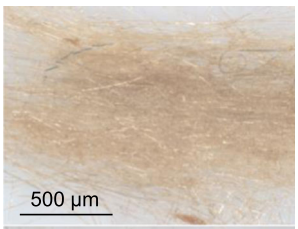
3D	Aqua	Halo of partially missing figure on left hand side. Subsequently combined with sample 5D.	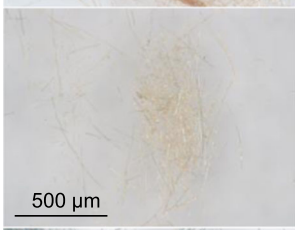
4D	Dark blue	Halo of partially missing figure on left hand side.	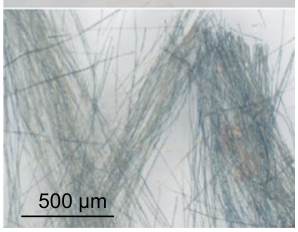
5D	Aqua	Halo of partially missing figure on left hand side. Subsequently	Not available

Table 1 (continued)

		combined with sample 3D.	
6D	Dark blue	Halo of the partially missing figure on the left hand side.	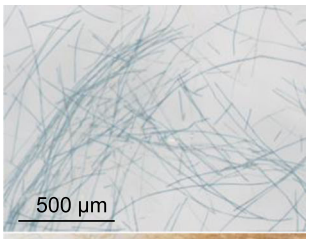
7D	Yellow	Darkest yellow stripe of halo of partially missing figure on left hand side.	
8D	Creamy yellow	Halo of partially missing figure on left hand side (the stripe was slightly lighter for sample 7D)	
9D	Pale yellow	Face of partially missing figure on left hand side.	
10D	Pale yellow	Neck of partially missing figure on left hand side.	
11D	Red/orange	Sash of first figure on left hand side.	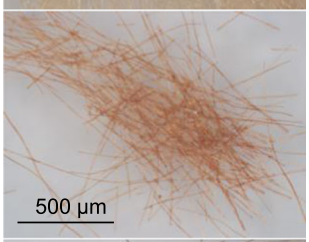
12D	Light brown	Dark area probably representing part of missing robe of second figure on left hand side.	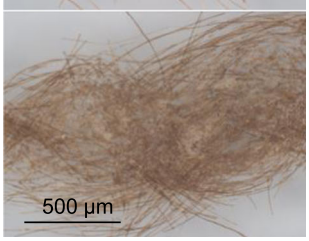

Table 1 (continued)

13D	Brown	Outline of the rocks/waterfalls surrounding the Buddha.	
14D	Light pink	One of the veils of the apsara in top left corner.	
15D	Yellow	One of the decorative waves surrounding the apsara in top left corner.	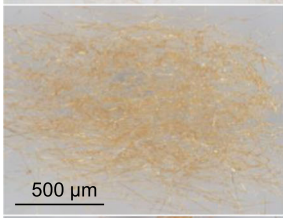
16D	Light pink	Lips of partially missing figure on right hand side.	
17D	Yellow	Robe of partially missing figure on right hand side.	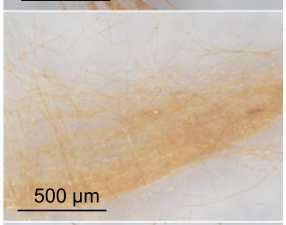
18D	Brown	Hair of one of the sitting figures in the bottom corner (right hand side).	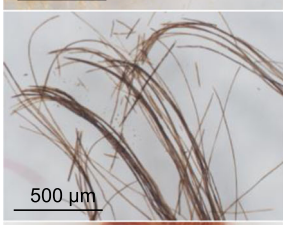
19D	Red	Robe of the Buddha (knot from back of textile).	
20D	Pink	One of the stripes of halo of the Buddha (back of the textile).	

Table 1 (continued)

21D	Green	One of the veils of the small figure in the top left corner (knot from back of textile).	
22D	Dark green	One of the decorative waves surrounding the apsara in the top left corner (back of the textile).	
23D	Red/orange	Sash of first figure on left hand side (back of textile).	
24D	Light green	Upper part of robe of first figure on left hand side (back of textile).	
25D	Purple	Stripe in robe of the Buddha (knot from back of textile). Only area where this colour is present	

95% A, followed by a linear gradient to 100% B in 10 min, and held for 2 min. Re-equilibration time for each analysis was 10 min. The ESI operating conditions were: drying gas N_2 (purity > 98%) at 350 °C and 10 L/min; capillary voltage 4.0 kV; nebuliser gas 40 psig and sheath gas N_2 (purity > 98%) at 375 °C and 11 L/min.

High-resolution MS and MS/MS spectra were acquired in negative mode in the range 100–1700 *m/z*. The fragmentor was kept at 150 V, nozzle voltage 1000 V, skimmer 65 V, octapole RF 750 V. For the MS/MS experiments, different voltages in the collision cell were tested for collision-induced dissociation (CID), in order to maximise the information obtained from the fragmentation. The collision gas was nitrogen (purity 99.999%). The data were collected by targeted MS/MS acquisition with an MS scan rate of 1.0 spectra/s and a MS/MS scan rate of 1.0 spectra/s. MassHunter® Workstation Software was used to carry out mass spectrometer control, data acquisition and data analysis.

The identification of the molecules in the samples was based on the comparison of the retention times and MS/MS spectra of reference molecules present in the BM database. When a reference molecule was not available, literature data were used (Degano et al. 2009; Han et al. 2017; Rosenberg 2008). In the case of unknown molecules, MS/MS spectra were acquired and discussion on possible structures is provided.

Chemicals and reagents

Dimethylsulphoxide (DMSO) (VWR, AnalaR NORMAPUR, purity > 99.5%), acetone (Fisher Chemical, pesticide residue grade, purity > 99.8%), oxalic acid dihydrate (VWR, AnalaR

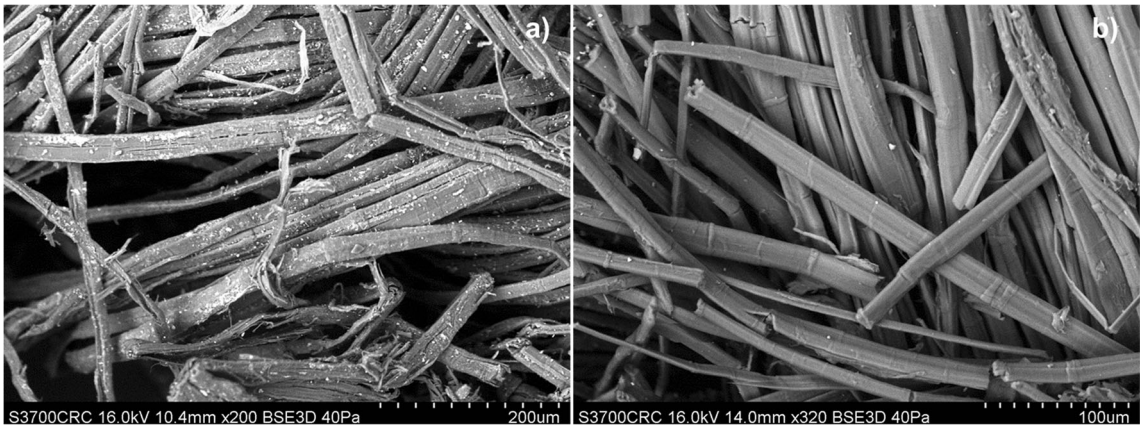

Fig. 3 VP SEM images of **a** hemp (*Cannabis sativa*) fibres (sample 1F), forming the original backing and **b** flax (*Linum usitatissimum)* fibres (sample 15F) from the restoration backing. Images: C.R. Cartwright © The Trustees of the British Museum

NORMAPUR, purity > 99.5%), methanol (Sigma Aldrich, HPLC grade, purity ≥ 99.9%), acetonitrile (VWR, HiPerSolv CHROMANORM, HPLC grade, purity ≥ 99.9%) and formic acid (Sigma Aldrich, eluent additive for LC-MS, purity 98–100%) were used as received. Water was used after purification by the PURELAB® Option-Q system.

Vials, inserts and pipette tips were all one-time use items, in order to prevent contamination.

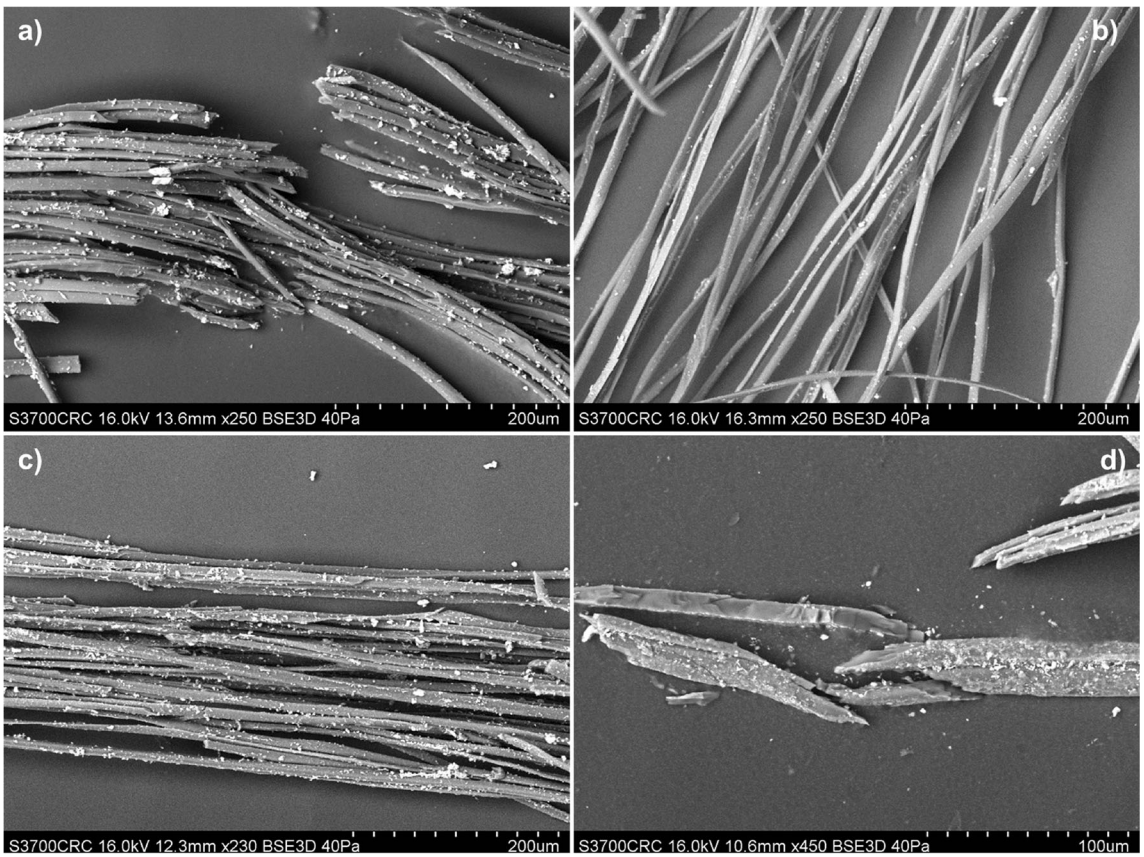

Fig. 4 VP SEM images of silk fibres of **a** sample 2F from the original embroidery, showing very brittle silk threads; **b** sample 14F from the original embroidery (cream rock) showing silk threads in better condition; **c** sample 6F from light blue embroidery, showing rather worn silk threads with much particulate matter and fragmentation in long lengths; **d** sample 11F from brown rocks area of embroidery, showing highly degraded, fragmented and brittle silk threads. Images: C.R. Cartwright © The Trustees of the British Museum

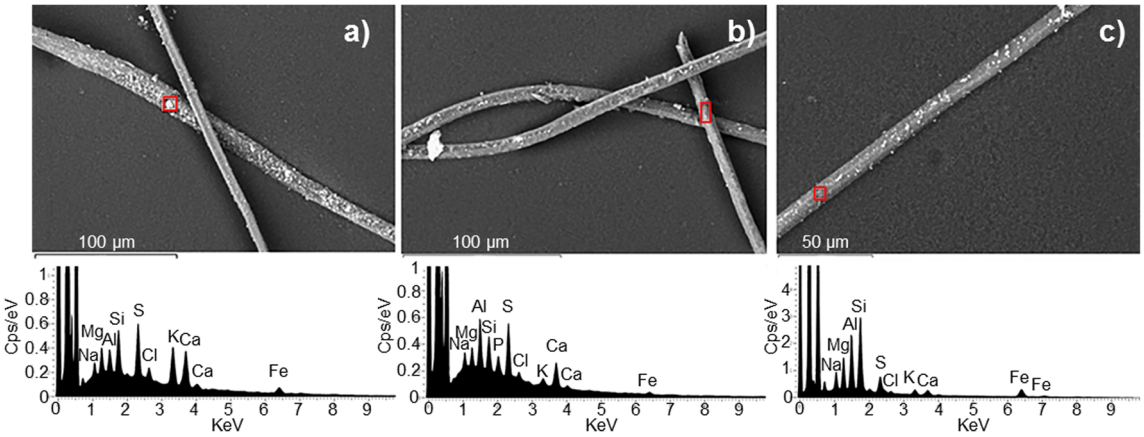

Fig. 5 SEM images of fibres from samples showing **a** 22D, a contaminated area, **b** 25D, an alum-mordanted fibre and **c** 18D, an iron-mordanted fibre. The areas were EDX spectra were acquired are shown as red squares. The EDX spectra are reported under the corresponding image. © The Trustees of the British Museum

Results

Fibre characterisation

In order to inform the conservation process, VP SEM identification was undertaken of fibre samples from (a) the original backing and patch lining and (b) the restoration backing (ca. 1912); these were confirmed to be (a) hemp (*Cannabis sativa*) (Fig. 3a) and (b) linen (*Linum usitatissimum*, flax) (Fig. 3b). The flax fibres showed several signs of degradation, mainly in the form of transverse cracks and fragmentation at dislocations. This confirmed the need to replace the restoration backing.

The principal fibre used for the embroidery was confirmed to be silk, but the condition of the silk threads varied considerably in different parts of the object. Sample 2F, ground silk, shows very brittle fibres (Fig. 4a), whereas sample 14F, from cream rock embroidery, shows the silk in better condition (Fig. 4b). Sample 6F, from light blue embroidery, displays rather worn silk threads with considerable particulate matter (Fig. 4c). In a similar way to sample 9F, from dark blue embroidery, this sample shows a tendency for the silk fibres to fragment in long lengths, but the condition of each silk fibre is not in an advanced state of degradation, unlike sample 11F from the brown rocks, which is both highly degraded, fragmented and brittle (Fig. 4d).

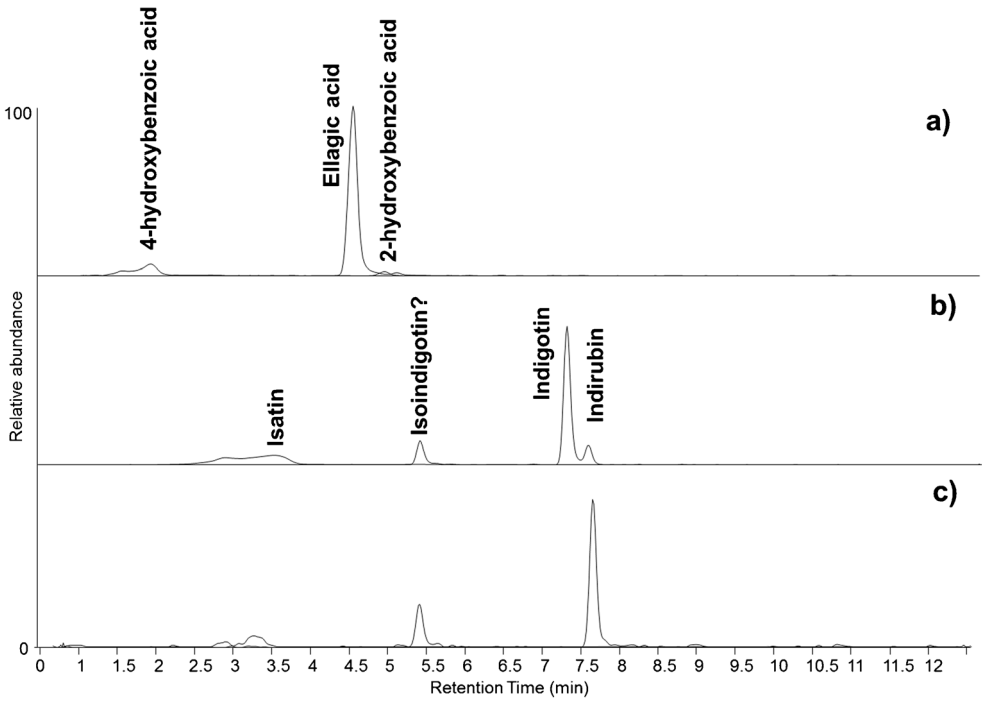

Fig. 6 Extract ion chromatographic profiles obtained by HPLC-ESI-Q-ToF analysis of samples **a** 18D (brown, negative ionisation mode), **b** 4D (blue, positive ionisation mode) and **c** 6D (blue, positive ionisation mode). © The Trustees of the British Museum

Mordant analysis

Most of the fibres analysed appeared partially covered by particles of dust or sand. The EDX spectra recorded on the particles revealed the presence of several elements, such as Al, Si, Fe, Ca, K, Cl, S, Mg, P and Na (Fig. 5a).

The investigation of mordants in archaeological textiles is a complicated subject, as elemental contamination makes the interpretation of the results difficult. In particular, the presence of Fe and Al as contaminants sometimes prevents conclusive information from being obtained, as these are the only marker elements for the detection of alum- and iron-mordanting processes. However, in our case, some less contaminated areas of the fibres were identified and it was possible to record spectra in these areas (Fig. 5b). Although contamination was still present, the relative abundances of the peaks corresponding to certain elements were used to identify the presence of mordants, in agreement with some guidelines described in the literature (Koestler et al. 1985; Rodríguez et al. 2013). In particular, the ratio between the heights of Al and Si signals was approximately 0.5 in all the clearly contaminated areas, whereas it was above 1 in some 'clear' areas, as shown in Fig. 5a, b, respectively. When this occurs, the fibre can be considered alum-mordanted (Koestler et al. 1985; Rodríguez et al. 2013). This was observed for samples 25D (purple), 23D (red) and 19D (red).

Indications of iron-mordanting were only found in sample 18D (brown) (Fig. 5c), as the abundance of Fe was generally much higher than observed in the contaminating particles. This was consistent with the colour and particularly poor preservation state of these fibres, as Fe is known to accelerate fibre degradation (Kohara et al. 2000).

Samples 22D (green), 20D (pink), 17D (yellow) and 4D (blue) appeared not to contain mordants, suggesting the use of direct and/or vat dyes.

Dye analysis

Brown

Three brown samples were analysed (12D, 13D and 18D) and the same chromatographic profiles were obtained, as shown in Fig. 6a.

Ellagic acid was identified as the most abundant compound. This molecule is a marker for tannin-based dyes. As it is sometimes the case in archaeological textiles, no other tannin-derived molecules were detected, making it impossible to identify the exact botanical source of the tannins used, although the literature reports the use of acorn cup (*Quercus acutissima*) as one of the most common sources to obtain browns (Han et al. 2017). 4-Hydroxybenzoic acid and 2-hydroxybenzoic acid were also identified. These compounds are sometimes identified as degradation products of tannins (Degano et al. 2011). However, in this case, they were present in all the samples analysed. Hydroxybenzoic acids are also reported to be degradation products of silk (Degano et al. 2011), this conclusion being more likely considering the poor preservation state of the silk embroidery threads.

Blues

Two dark blue samples (4D and 6D) with slightly different shades were analysed. Indigo (as a general term) is always the source of blue colours in naturally dyed textiles (Cardon 2007; Puchalska et al. 2004; Rosenberg 2008), and isatin, indigotin and indirubin are usually found as the main dye components (Han et al. 2017; Puchalska et al. 2004). In our samples two different chromatographic profiles were obtained, as shown in Fig. 6b, c.

Sample 4D showed the presence of isatin, indigotin and indirubin, with indigotin being the most abundant peak (Table 2). A fourth compound was present with the same mass as indigotin and indirubin $[M + H]^+ = 263.0815$ u. The MS/MS spectrum of this compound showed many similarities with the MS/MS spectrum of indigotin (Fig. S2, Supplementary material). The fragment ions $[M + H–18]^+$, $[M + H–28]^+$, $[M + H–46]^+$ and $[M + H–73]^+$, corresponding to $[M + H–H_2O]^+$, $[M + H–CO]^+$, $[M + H–CO–H_2O]^+$ and $[M + H–CO–NH_2–H_2O]^+$, respectively, were present. This suggested that the compound is probably the indigotin isomer isoindigotin (Maugard et al. 2001; Puchalska et al. 2004).

This compound was also present in the chromatogram obtained for sample 6D, as well as isatin and indirubin. However, the chromatographic peak for indigotin showed an extremely low abundance in this sample compared to indirubin. One reason for this difference may be that two different sources of indigo were used. In fact, several indigo-producing plants are reported in the literature as possible blue sources in Asia. In addition to the cultivated *Indigofera tinctoria*, originating in India, and the relatively common woad (*Isatis tinctoria*), *Polygonum tinctorium* and *Strobilanthes cusia* (syn. *Baphicacanthus cusia*) have been reported as traditional Chinese sources for dyeing blue (Cardon 2007; De Luca et al. 2016; Grzywacz et al. 2004). All these plants yield approximately the same dye components; therefore, it is difficult to differentiate between them based on the chemistry alone. Furthermore, different dyeing techniques or different degradation pathways may also have produced the observed differences.

Indigo was also detected in all the green samples (3D, 5D, 21D, 22D, 24D). Mixed blue and yellow fleeces or subsequent dyeing were used to obtain different shades, from aqua to dark green. The distribution of the blue dye components in samples 3D, 5D, 21D and 24D was similar to what obtained for sample

Table 2 Summary of the results obtained from the dye analysis of the samples by HPLC-ESI-Q-ToF

Sample name	Colour	Dye molecules	Possible sources
1D	Pale yellow	None	
2D	Pale yellow	Berberine, Berberine oxidation product	*P. chinense*
3D	Aqua	Isatin, indigotin, indirubin, isoindigotin Berberine, Berberine oxidation product	Blue: *I. tinctoria**, *P. tinctorium, S. cusia* (syn. *B. cusia*) Yellow: *P. chinense*
4D	Dark blue	Isatin, indigotin, indirubin, isoindigotin	*I tinctoria**, *P. tinctorium, S. cusia*
5D	Aqua	Isatin, indigotin, indirubin, isoindigotin Berberine, Berberine oxidation product	Blue: *I. tinctoria**, *P. tinctorium, S. cusia* Yellow: *P. chinense*
6D	Dark blue	Isatin, indigotin (very low), indirubin, isoindigotin	*I. tinctoria**, *P. tinctorium, S. cusia*
7D	Yellow	Berberine, Berberine oxidation product	*P. chinense*
8D	Creamy yellow	Luteolin, Apigenin, Luteolin-4-O′-glucoside, Apigenin-7-glucoside, Luteolin-7-glucoside	*R. luteola*
9D	Pale yellow	None	
10D	Pale yellow	None	
11D	Red/orange	Luteolin, Apigenin, Emodin Not fully identified molecules (anthraquinones, polyhydroxyanthraquinones, etc.)	Unknown
12D	Light brown	Ellagic acid	Tannin-based
13D	Brown	Ellagic acid	Tannin-based
14D	Light pink	None	
15D	Yellow	Berberine, Berberine oxidation product	*P. chinense*
16D	Light pink	None	
17D	Yellow	Berberine, Berberine oxidation product	*P. chinense*
18D	Brown	Ellagic acid	Tannin-based
19D	Red	Anthragallol, Alizarin, Purpurin Pseudopurpurin, Xanthopurpurin, Munjistin, Rubiadin, Nordamnacantha, 6-hydroxyrubiadin (?)	*Rubia* spp.
20D	Pink	Carthamin, Carthamin degradation products, Ct component Luteolin, Apigenin, Chrysoeriol, *O*-methylated flavone Luteolin-glucuronide, Apigenin-glucuronide, Chrysoeriol-glucuronide, *O*-methylated flavone-glucuronide	*C. tinctorius* Unknown yellow
21D	Green	Isatin, indigotin, indirubin, isoindigotin Luteolin, Apigenin, Luteolin-4-O′-glucoside, Apigenin-7-glucoside, Luteolin-7-glucoside Berberine, Berberine oxidation product	*I. tinctoria**, *P. tinctorium, S. cusia* *P. chinense* *Reseda luteola (?)*
22D	Dark green	Isatin, indigotin (very low), indirubin, isoindigotin Berberine oxidation product	*I. tinctoria**, *P. tinctorium, S. cusia* *P. chinense*
23D	Red/orange	Luteolin, Apigenin, Emodin Not fully identified molecules (anthraquinones, polyhydroxyanthraquinones, etc.)	Unknown
24D	Light green	Isatin, indigotin, indirubin, isoindigotin Berberine oxidation product	*I. tinctoria**, *P. tinctorium, S. cusia* *P. chinense*
25D	Purple	Shikonin Brazilin, type C component, Emodin Not fully identified molecules (polyhydroxyxanthones?)	*L. erythrorhizon, C. sappan*

*Both *Indigofera tinctoria* and *Isatis tinctoria* as possible sources

4D (Fig. 6b), whereas the results for sample 22D revealed a high relative abundance of indirubin, more similar to sample 6D (Fig. 6c), pointing towards the hypothesis that the two sources of indigo were also used for the green colours.

Yellows

Several yellow samples from different locations were analysed. Some of them showed a pale colour (samples 1D, 2D, 8D, 9D and 10D), whereas others were brighter (samples

7D, 15D, 17D). With regard to the 'pale' samples, only samples 2D and 8D were found to contain dye molecules. Samples 1D, 9D and 10D were all taken from the skin of the partially missing figure on the left hand side (Table 1). After cleaning of the textile, these areas appeared lighter in colour and would not be defined as 'pale yellows', but rather undyed, in agreement with the HPLC-MS results.

Samples 2D and 8D showed two different dye compositions. Berberine was detected in sample 2D (Fig. 7a). Luteolin, apigenin and some of their glycosides were detected in sample 8D (Fig. 7b). All the 'darker' samples (samples 7D, 15D, 17D) showed the same composition as sample 2D, with berberine as the main component.

Plant materials containing protoberberine alkaloids have been used commonly in Asia since ancient times. Among these plants, amur cork tree (*Phellodendron amurense* in Japan and *P. chinense* in China), goldthread (*Coptis japonica* in Japan and *C. chinensis* in China), Japanese barberry (*Berberis thunbergii*) and huangteng (*Fibraurea tinctoria*) are the best documented (Gibbs et al. 1997; Grzywacz et al. 2004; Han et al. 2017; Sasaki and Sasaki 2013; Zhang et al. 2007). All these plants contain berberine as the main alkaloid, except huangteng, in which berberine is absent (Sasaki and Sasaki 2013; Zhang et al. 2007). Both Japanese and Chinese goldthreads are distinguishable by the presence of coptisine, whereas the various amur cork trees and Japanese barberry contain small amounts of palmatine and jatrorrhizine relative to berberine (Gibbs et al. 1997; Sasaki and Sasaki 2013).

In our case, all the samples containing berberine showed the presence of a second alkaloid. The high-resolution mass measurements allowed us to identify the compound as a berberine oxidation product. In fact, the measured mass of the detected compound was 352.1179 u, compatible with the chemical formula $C_{20}H_{18}NO_5^+$ and not to be mistaken with the exact mass for palmatine ($C_{21}H_{22}NO_4^+$), which is 352.1549 u. This chemical formula corresponds to the formula of berberine ($C_{20}H_{18}NO_4^+$) with one additional oxygen atom. In addition, the MS/MS spectrum of the compound (Fig. S3, Supplementary material) clearly highlighted that the fragmentation pattern was the same as berberine with +16 u difference for all the fragment ions. The position of the oxygen atom, whether in a hydroxyl or keto functionality, was not ascertained from these results.

The absence of any other alkaloid was not in agreement with most of the literature (Gibbs et al. 1997; Sasaki and Sasaki 2013; Zhang et al. 2007), but a high variability of results can be found in these works and some yellow paper samples from Dunhuang (eighth century AD) containing only berberine were found (Gibbs et al. 1997). The authors suggested that a plant extract other than *Phellodendron amurense* or *P. chinense* (the most common in China) may have been used at that time. In addition, palmatine content in *P. amurense* is reported to vary depending on which part of the tree it is obtained from (Sasaki and Sasaki 2013) and degradation phenomena should be taken into consideration, as well as dye bath conditions.

As regards the luteolin-based source of yellow dye, the composition was similar to the one commonly obtained for weld (*Reseda luteola*), except for a very weak signal obtained for chrysoeriol, considered as one of the weld biomarkers

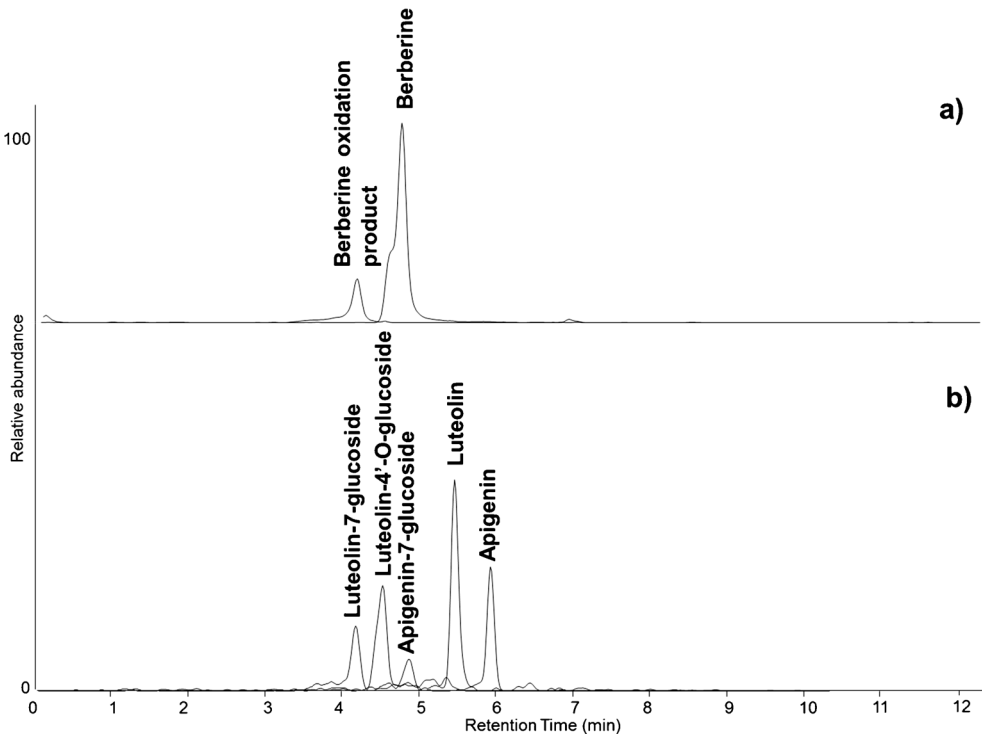

Fig. 7 Extract ion chromatographic profiles obtained by HPLC-ESI-Q-ToF analysis of yellow samples **a** 2D (positive ionisation mode) and **b** 8D (negative ionisation mode). © The Trustees of the British Museum

(Peggie et al. 2008). A similar result has been obtained by Zhang et al. (Zhang et al. 2008). However, as also underlined by those authors, weld is not a typical Chinese plant at present, though it may have been in the past. Some other unknown Asian sources of luteolin might have been used in these cases.

The green samples (3D, 5D, 21D, 22D, 24D) also contained these two types of yellow dyes. Sample 21D contained a mixture of berberine and the luteolin-based dye, whereas all the other samples contained berberine.

The photophysical properties of protoberberines have been extensively studied and their characteristic yellow/greenish UV-induced luminescence is known (Diaz et al. 2009; Megyesi and Biczók 2007). The results are therefore in agreement with the information obtained during the visual examinations ('Visual examinations' section, Fig. 2), where one fluorescent and one non-fluorescent source of yellow were observed.

Pink

Three samples were classified as pink (samples 14D, 16D and 20D). Dye molecules were only detected and identified in sample 20D, as shown in Fig. 8. Carthamin and the two degradation products of carthamin ($[M\text{-}H]^-$ = *m/z* 477.1038 corresponding to $C_{22}H_{22}O_{12}$, and $[M\text{-}H]^-$ = *m/z* 449.1084 corresponding to $C_{21}H_{22}O_{11}$), identified by Laursen and Mouri (Laursen and Mouri 2013) were present. In addition, one of the so-called Ct components (*m/z* 582.2615) was detected (Wouters et al. 2010). These compounds are all markers of safflower (*Carthamus tinctorius*), known to be a very light-sensitive dye, which explains the presence of a vibrant pink on the back of the textile but not on the front. Also in this case, dye analysis supported the information obtained by visual examination under UV light, where an orange fluorescence, potentially in agreement with safflower (Nakamura et al. 2014), was observed in some faded areas ('Visual examinations'section, Fig. 2).

In addition to the main markers of safflower, four flavonoids were identified in sample 20D, namely apigenin, luteolin, chrysoeriol and an *O*-methylated flavone, whose mass corresponded to chrysoeriol without one hydroxyl group. There are many flavonoids corresponding to this structure, such as acacetin, methyl-genistein, genkwanin, glycitein, etc. The MS/MS spectrum of the compound did not allow us to assign an exact chemical structure to this molecule, as the spectrum was dominated by the fragment ion arising from the loss of the methyl group. Although apigenin and chrysoeriol have been detected in safflower samples (Wouters et al. 2010), the distribution of the four flavonoids in this sample, with chrysoeriol as the most abundant one, did not match any common source of flavonoid dyes. Moreover, the four flavonoids were all also found in the form of O-glucuronide derivatives. The MS/MS spectra showed a main fragmentation peak corresponding to the loss of 176 u, which is the main fragmentation reported when O-glucuronide flavonoids are present (Marczak et al. 2016) (Fig. S4, Supplementary material).

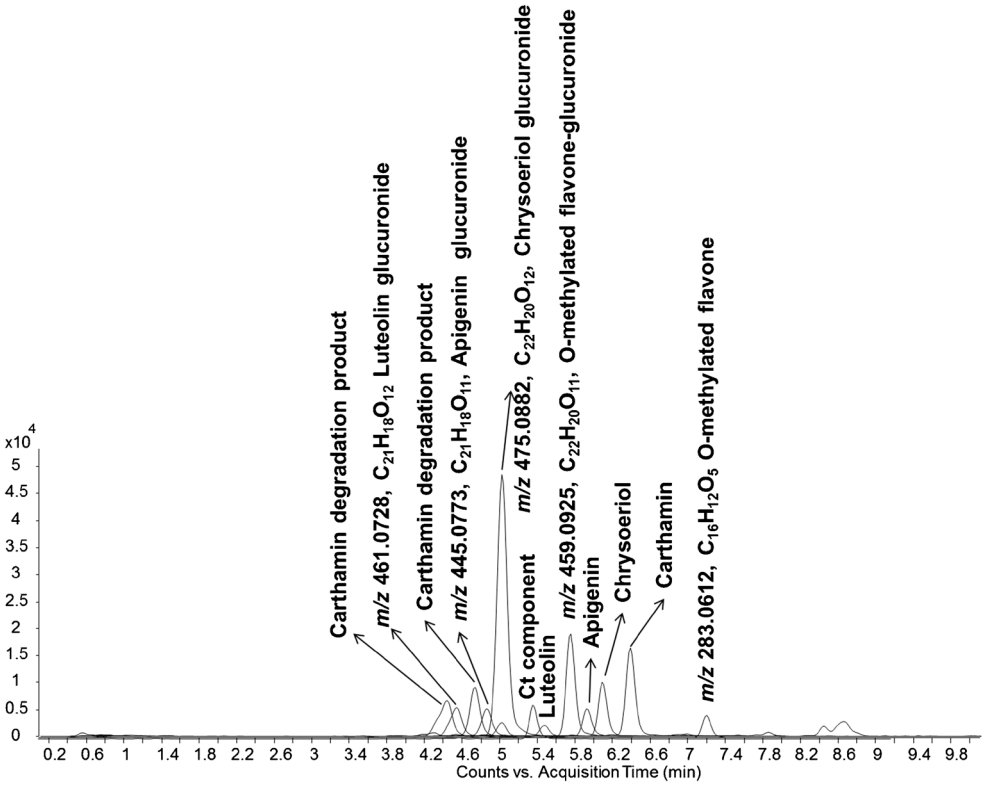

Fig. 8 Extract ion chromatographic profile obtained by HPLC-ESI-Q-ToF analysis of pink sample 20D (negative ionisation mode). Experimental mass values of the deprotonated molecules $[M\text{-}H]^-$ and corresponding chemical formulas of the O-glucuronide flavonoids are reported. © The Trustees of the British Museum

Luteolin-glucuronide has been suggested as a possible component in some Chinese samples from Zaghunluq (Xinjiang) by Zhang et al. (Zhang et al. 2008). Glucuronide derivatives of flavonoids are present in several plants, but have not been commonly identified as dye components. Although this does not exclude their presence as part of an unknown yellow dye, another hypothesis could be formulated. In fact, dyeing pink/red with safflower requires the adjustment of the pH of the dye bath and natural products were used to do this in ancient times. The use of dark plum juice is reported (Han 2016), but other substances or processes could have been used, resulting in the detection of these unusual compounds.

Purple

One purple sample (sample 25D) was analysed, whose chromatographic profile revealed the presence of various dye molecules (Fig. 9).

Shikonin is considered the molecular marker for the presence of gromwell (*Lithospermum erythrorhizon*) (Cardon 2007; Han et al. 2017) and was identified in the sample. However, other Boraginaceae plants from Asia contain shikonin and/or alkannin (its stereoisomer) as main dye molecule (Cardon 2007). The MS/MS spectrum of shikonin (Fig. S5, Supplementary material) shows the typical fragment ion at *m/z* 218.0221, which results from the cleavage of the molecule at the benzylic position.

Brazilin was also identified, despite the very low abundance, and was considered as an indication of the presence of sappan wood, *Caesalpinia sappan* (*Biancaea sappan*). The identification of sappan wood by means of HPLC analysis does not usually rely on the detection of brazilein and/or brazilin, which are fugitive and unstable compounds, but rather on the detection of the so-called 'type C compound' (Karapanagiotis et al. 2009; Karapanagiotis et al. 2011; Manhita et al. 2011; Nowik 2001). Although this compound can be identified by the corresponding UV-visible absorption spectrum, its chemical structure and formation mechanism are not known.

In our analysis the 'type C compound' was identified and showed a mass value of the deprotonated molecule 243.0299 u, in agreement with Manhita et al. (2011). The molecule, confirmed to be also present in a reference of silk dyed with sappan wood, was consistent with the chemical formula $C_{13}H_8O_5$ and produced a MS/MS spectrum consistent with a trihydroxyxanthone. Although trihydroxyxanthone was not present in our reference database, the spectrum showed many similarities with the one obtained for euxanthone ($C_{13}H_8O_4$, dihydroxyxanthone), which was present in our database. In fact, most of the fragment ions showed a + 16 u difference, indicative of an additional oxygen atom, but the fragmentation pattern was mostly the same (Fig. S6, Supplementary material). A second compound, whose deprotonated molecule mass was at *m/z* 259.0248 and consistent with the chemical formula $C_{13}H_8O_6$, showed a similar MS/MS spectrum. Also in this case, the fragmentation showed a + 16 u difference for most of the fragment ions (Fig. S6, Supplementary material). This led us to hypothesise the structure of a tetrahydroxyxanthone for this compound. This compound was not present in the reference of silk dyed with sappan wood, but can be seen as an oxidation product of the 'type C compound'.

Xanthones have been reported as components of sappan wood (Nirmal et al. 2015); therefore, based on these results,

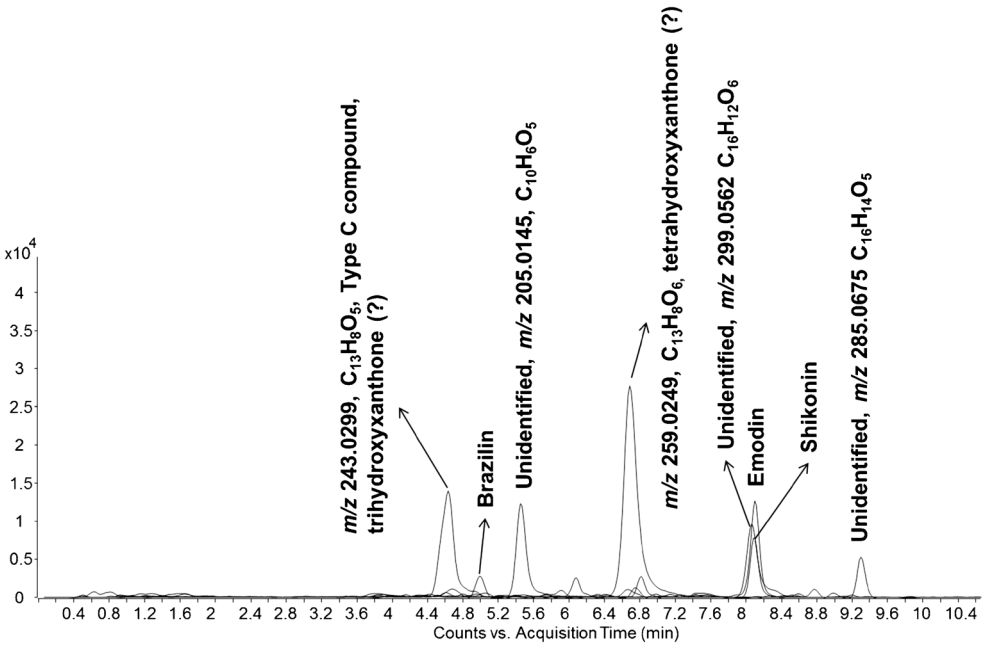

Fig. 9 Extract ion chromatographic profile obtained by HPLC-ESI-Q-ToF analysis of purple sample 25D (negative ionisation mode). Experimental mass values and corresponding chemical formulas of the detected molecules are reported. © The Trustees of the British Museum

we hypothesise that these compounds can be used as diagnostic markers for the presence of sappan wood. In addition, although it has been suggested that the 'type C compound' may derive from the ageing of the dye due to exposure to light (Manhita et al. 2011), we suggest here that it could have the structure of a trihydroxyxanthone, thus would not be directly related to the structure of brazilein.

Emodin, a very common molecule found in many plants (Cardon 2007), and a few other unidentified molecules were also detected in the sample.

Reds

Three red samples were analysed, corresponding to two different red colours: a more orange/brownish red (samples 11D and 23D) and a bright red (sample 19D).

Anthraquinones attributable to the dye composition of a Rubiaceae plant (madder) were detected in sample 19D (bright red). In particular, anthragallol, alizarin, purpurin pseudopurpurin, xanthopurpurin, munjistin, rubiadin and nordamnacanthal were identified, as shown in Fig. 10a.

The relatively high abundance of munjistin points towards *Rubia cordifolia* (munjeet or manjishtha) used as possible plant source for the madder (Mouri and Laursen 2012; Wouters 1985; Wouters et al. 2011). However, low relative abundances of alizarin and rubiadin are generally derived from this plant, not fully in agreement with our results. Additionally, 6-hydroxyrubiadin has been reported as marker for the *R. akane* (Japanese madder) (Mouri and Laursen 2012), but it has also recently been indicated as marker for *R. cordifolia* in non-aged samples (Han et al. 2017). In our analysis, 6-hydroxyrubiadin was tentatively identified as a minor component compared to the other anthraquinones, making the attribution to a botanical source extremely challenging, as it usually occurs when dealing with ancient samples.

The results obtained from the other two samples were much more difficult to interpret. Luteolin and apigenin were

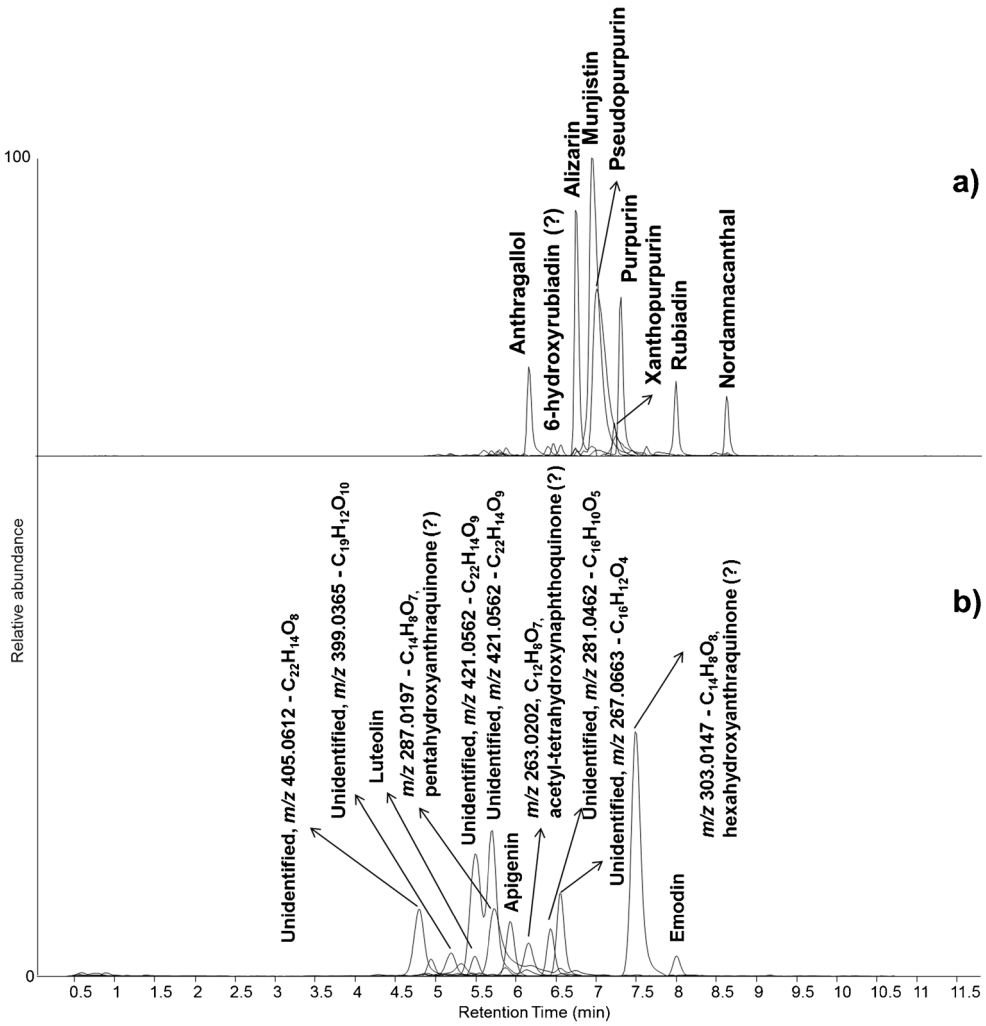

Fig. 10 Extract ion chromatographic profiles obtained by HPLC-ESI-Q-ToF analysis of red samples **a** 19D (negative ionisation mode) and **b** 23D (negative ionisation mode). Experimental mass values and corresponding chemical formulas of the detected molecules are reported. © The Trustees of the British Museum

detected (Fig. 10b), suggesting that a source of yellow flavonoids was present in the sample. The anthraquinone emodin was identified as well. Several other molecules were detected, but not clearly identified.

The MS/MS spectra of three of the unknown compounds, whose deprotonated molecule masses were 263.0197, 287.0197 and 303.0146 u, respectively, showed some similarities (Fig. S7, Supplementary material), as they were dominated by $[M-H-18]^-$ and $[M-H-28]^-$ fragment ions, in a similar way to what happens to anthraquinone/naphthoquinone molecules. The masses were compatible with the chemical formulas $C_{12}H_8O_7$, $C_{14}H_8O_7$ and $C_{14}H_8O_8$ and the fragmentation patterns showed a good match (over 80%) with acetyltetrahydroxynaphthoquinone (or spinochrome A), pentahydroxyanthraquinone and hexahydroxyanthraquinone, respectively. The tentative assignment of these molecular structures is based on the fragmentation pathways observed, but is not confirmed by reference molecules due to the lack of standards (further investigations are on-going).

For two other unknown molecules, the masses of the deprotonated molecules were 267.0663 and 281.0455 u, respectively, compatible with chemical formulas $C_{16}H_{12}O_4$ and $C_{16}H_{10}O_5$, respectively. It was possible to ascertain the presence of at least one methyl group in the former molecule, as the MS/MS spectrum was dominated by the fragment ion with $[M-H-15]^-$, whereas the MS/MS spectrum of the latter molecule showed a $[M-H-28]^-$ fragment ion (Fig. S8, Supplementary material). This made further considerations on their structures difficult to be obtained.

The MS/MS spectra of two other unknown compounds showed similarities (Fig. S9, Supplementary material). The masses of the deprotonated molecules for these compounds were 405.0616 and 421.0565 u, respectively. The latter one was present in two isomeric forms. The masses were compatible with chemical formula $C_{22}H_{14}O_8$ and $C_{22}H_{14}O_9$, respectively. The fragmentations showed fragment ions with $[M-H-28]^-$ and $[M-H-44]^-$, corresponding to CO and COOH losses. Fragment ions with high abundance were found at *m/z* 243.0297 and 259.0246, respectively, corresponding to the ions $[M-H-162]^-$ and suggesting the presence of a glucose molecule, but the elucidation of the entire mass spectra remains challenging. The nature and the source of this red dye are unknown at this stage of the investigation, highlighting that research still needs to be done to identify Asian colourants in archaeological textiles.

Conclusions

SEM-EDX and HPLC-ESI-Q-ToF were used to investigate a high number of samples from the Chinese embroidery 'Sakyamuni Preaching on Vulture Peak' focusing on fibre characterisation, indications about the use of mordants and identification of dyes.

The results confirmed the use of different types of fibres (hemp, linen and silk) in different parts of the panel and highlighted their poor degradation state in most cases. The use of an alum mordant in relation to red anthraquinones and purple naphthoquinones was detected and an iron mordant was found associated with the use of tannins. The other dyes (pink, yellows, blue and greens shades) were mostly applied as direct and/or vat dyes.

The identification of the dyes has expanded the database of literature data on ancient Chinese dyes in textiles from the Silk Road, which remains a relatively poorly investigated subject, especially in terms of application of HPLC-ESI-Q-ToF. In addition to the identification of expected dye sources, such as a berberine-based yellow (most likely *P. chinense*), *Rubia* spp. for the red, *C. tinctorius* for the pink, the results also highlighted new insights into the use of dyes. In particular, a mixture of shikon (*L. erythrorhizon*) and sappanwood (*C. sappan*) to obtain a particular purple shade, and the probable use of more than one source of indigo were highlighted. Some limitations were also revealed, especially regarding the identification of some uncommon sources of yellow and red dyes. This is mainly due to the lack of reference materials, MS/MS data and information about degradation. In an attempt to overcome these limitations, a selection of dye plants from China has been collected at the British Museum and is being used to build a database of MS/MS data of dye molecules. This, together with some comparative work involving other textiles from Dunhuang, will enhance the possibilities of identification of Chinese dyes in archaeological textiles.

Acknowledgements The authors would like to thank the Queen Elizabeth Scholarship Trust (QEST) for funding Hannah Vickers' internship at the British Museum. The conservation work was also supported by the Idlewild Trust, the Thriplow Charitable Trust and the Nara National Museum. Monika Harter (former Head of Organics, Department of Conservation, British Museum), Yu-Ping Luk (Curator, Asia Department, British Museum) and Jane Portal (Keeper, Asia Department, British Museum) are thanked for their involvement in the project and useful discussions. As an Andrew W. Mellon Postdoctoral Research Fellow, Diego Tamburini would like to thank the Andrew W. Mellon Foundation.

References

Cardon D (2007) Natural dyes. Sources, tradition, technology and science. Archetype Publications Ltd., London

Cave Temples of Dunhuang (2016) Buddhist art on China's silk road. The Getty Conservation Institute, Los Angeles

Cave Temples of Mogao at Dunhuang (2015) Art and history on the silk road. The Getty Conservation Institute, Los Angeles

Conservation of Ancient Sites on the Silk Road (1997). The Getty Conservation Institute, Los Angeles

Conservation of Ancient Sites on the Silk Road (2010) vol 2. The Getty Conservation Institute, Los Angeles

The Conservation of Cave 85 at the Mogao Grottoes, Dunhuang (2013). The Getty Conservation Institute, Los Angeles

De Luca E, Poldi G, Redaelli M, Zaffino C, Bruni S (2016) Multi-technique investigation of historical Chinese dyestuffs used in Ningxia carpets. Archaeological and Anthropological Sciences:1–10. https://doi.org/10.1007/s12520-016-0334-z

Degano I, Biesaga M, Colombini MP, Trojanowicz M (2011) Historical and archaeological textiles: an insight on degradation products of wool and silk yarns. J Chromatogr A 1218(34):5837–5847. https://doi.org/10.1016/j.chroma.2011.06.095

Degano I, La Nasa J (2016) Trends in high performance liquid chromatography for cultural heritage. Top Curr Chem 374(2):1–28. https://doi.org/10.1007/s41061-016-0020-8

Degano I, Ribechini E, Modugno F, Colombini MP (2009) Analytical methods for the characterization of organic dyes in artworks and in historical textiles. Appl Spectrosc Rev 44(5):363–410. https://doi.org/10.1080/05704920902937876

Diaz MS, Freile ML, Gutierrez MI (2009) Solvent effect on the UV/Vis absorption and fluorescence spectroscopic properties of berberine. Photochemical & Photobiological Sciences 8(7):970–974. https://doi.org/10.1039/b822363g

Dyer J, Tamburini D (2017) An unusual pink colorant found on a Hellenistic oinochoe (to be updated). Dyes and Pigments Forthcoming

Fan J, Yongzeng L (2007) Appreciation of Dunhuang Grottoes. Jiangsu Fine Arts Publishing House, Nanjing

Feng Z (2007) Textiles from Dunhuang in UK collections. Donghua University Press, Shanghai

Gibbs PJ, Seddon KR, Brovenko NM, Petrosyan YA, Barnard M (1997) Analysis of ancient dyed Chinese papers by high-performance liquid chromatography. Anal Chem 69(10):1965–1969. https://doi.org/10.1021/ac960279v

Grzywacz CM, Wouters J, Bomin S, Yuquan F (2004) Conservation of ancient sites on the silk road—Asian organic colourants: a collaborative research project. In: Agnew N (ed) Second International Conference on the Conservation of Grotto Sites, Mogao Grottoes, Dunhuang, China. Getty Conservation Institute

Gulmini M et al. (2016) The "Coptic" textiles of the "Museo Egizio" in Torino (Italy): a focus on dyes through a multi-technique approach. Archaeol Anthropol Sci:1–13. https://doi.org/10.1007/s12520-016-0376-2

Han J (2016) The historical and chemical investigation of dyes in high status Chinese costume and textiles of the Ming and Qing dynasties (1368–1911). University of Glasgow

Han J, Wanrooij J, van Bommel M, Quye A (2017) Characterisation of chemical components for identifying historical Chinese textile dyes by ultra high performance liquid chromatography–photodiode array–electrospray ionisation mass spectrometer. J Chromatogr A 1479:87–96. https://doi.org/10.1016/j.chroma.2016.11.044

Jolly A, Vanden Berghe I, Wouters J (2017) Europe or China? Dyestuff analyses as a tool for attributions. In: Kirby J (ed) The diversity of dyes in history and archaeology. Archetype Publications, London, pp 6–17

Karapanagiotis I, Minopoulou E, Valianou L, Daniilia S, Chryssoulakis Y (2009) Investigation of the colourants used in icons of the Cretan School of iconography. Anal Chim Acta 647(2):231–242. https://doi.org/10.1016/j.aca.2009.06.012

Karapanagiotis I, Theologou J, Lakka A, Ozoline A, Panayiotou C (2011) Investigation of the colouring materials of Fustat carpet fragments. Archaeometry 53(3):587–599. https://doi.org/10.1111/j.1475-4754.2010.00569.x

Karpova E, Vasiliev V, Mamatyuk V, Polosmak N, Kundo L (2016) Xiongnu burial complex: a study of ancient textiles from the 22nd Noin-Ula barrow (Mongolia, first century AD). J Archaeol Sci 70:15–22. https://doi.org/10.1016/j.jas.2016.04.001

Koestler RJ, Sheryll R, Indictor N (1985) Identification of dyeing mordants and related substances on textile fibers: a preliminary study using energy dispersive X-ray spectrometry. Stud Conserv 30(2):58–62. https://doi.org/10.2307/1506089

Kohara N, Sano C, Ikuno H, Magoshi Y, Becker MA, Yatagai M, Saito M (2000) Degradation and color fading of cotton Fabrics dyed with natural dyes and mordant. In: Historic textiles, papers, and polymers in museums, vol 779. ACS Symposium Series, vol 779. American Chemical Society, pp 74–85. https://doi.org/10.1021/bk-2001-0779.ch006

Laursen R, Mouri C (2013) Decomposition and analysis of carthamin in safflower-dyed textiles e-preservation. Science 10:35–37

Laursen R, Mouri C, Feng Z, Bo L, Jian L (2015) Section III—dyes in ancient Chinese and Japanese textiles. In: Dusenbury MM (ed) Color in ancient and medieval East Asia. Spencer Museum of Art, University of Kansas, Yale University Press, New Haven and London, pp 81–113

Lee J, Kang M, Lee K-B, Lee Y (2013) Characterization of natural dyes and traditional korean silk fabric by surface analytical techniques. Materials 6(5):2007–2025. https://doi.org/10.3390/ma6052007

Lombardi L, Serafini I, Guiso M, Sciubba F, Bianco A (2016) A new approach to the mild extraction of madder dyes from lake and textile. Microchem J 126:373–380. https://doi.org/10.1016/j.microc.2015.12.021

Manhita A, Ferreira T, Candeias A, Barrocas Dias C (2011) Extracting natural dyes from wool—an evaluation of extraction methods. Anal Bioanal Chem 400(5):1501–1514. https://doi.org/10.1007/s00216-011-4858-x

Marczak Ł, Znajdek-Awiżeń P, Bylka W (2016) The use of mass spectrometric techniques to differentiate isobaric and isomeric flavonoid conjugates from Axyris amaranthoides. Molecules 21(9):1229. https://doi.org/10.3390/molecules21091229

Maugard T, Enaud E, Choisy P, Legoy MD (2001) Identification of an indigo precursor from leaves of Isatis tinctoria (Woad). Phytochemistry 58(6):897–904. https://doi.org/10.1016/S0031-9422(01)00335-1

Megyesi M, Biczók L (2007) Effect of ion pairing on the fluorescence of berberine, a natural isoquinoline alkaloid. Chem Phys Lett 447(4-6):247–251. https://doi.org/10.1016/j.cplett.2007.09.046

Mouri C, Laursen R (2011) Identification and partial characterization of C-glycosylflavone markers in Asian plant dyes using liquid chromatography–tandem mass spectrometry. J Chromatogr A 1218(41):7325–7330. https://doi.org/10.1016/j.chroma.2011.08.048

Mouri C, Laursen R (2012) Identification of anthraquinone markers for distinguishing Rubia species in madder-dyed textiles by HPLC. Microchim Acta 179(1-2):105–113. https://doi.org/10.1007/s00604-012-0868-4

Nakamura R, Tanaka Y, Ogata A, Masakazu N (2014) Scientific evidence by fluorescence spectrometry for safflower red on ancient Japanese textiles stored in the Shosoin treasure house repository. Stud Conserv 59(6):367–376. https://doi.org/10.1179/2047058413y.0000000082

Nakamura R, Tanaka Y, Ogata A, Naruse M (2009) Dye analysis of Shosoin textiles using excitation−emission matrix fluorescence and ultraviolet−visible reflectance spectroscopic techniques. Anal Chem 81(14):5691–5698. https://doi.org/10.1021/ac900428a

Nirmal NP, Rajput MS, Prasad RGSV, Ahmad M (2015) Brazilin from Caesalpinia sappan heartwood and its pharmacological activities: a review Asian Pacific. Journal of Tropical Medicine 8(6):421–430. https://doi.org/10.1016/j.apjtm.2015.05.014

Nowik W (2001) The possibility of differentiation and identification of red and blue "soluble" dyewoods: determination of species used in dyeing and chemistry of their dyestuff. Paper presented at the Dyes in History and Archaeology 16/17, Lyons and Greenwich, 1997 and 1998

Pauk V, Barták P, Lemr K (2014) Characterization of natural organic colorants in historical and art objects by high-performance liquid

chromatography. J Sep Sci 37(23):3393–3410. https://doi.org/10.1002/jssc.201400650

Peggie AD, Hulme NA, McNab H, Quye A (2008) Towards the identification of characteristic minor components from textiles dyed with weld (Reseda luteola L.) and those dyed with Mexican cochineal (Dactylopius coccus Costa). Microchim Acta 162(3-4):371–380. https://doi.org/10.1007/s00604-007-0866-0

Puchalska M, Połeć-Pawlak K, Zadrożna I, Hryszko H, Jarosz M (2004) Identification of indigoid dyes in natural organic pigments used in historical art objects by high-performance liquid chromatography coupled to electrospray ionization mass spectrometry. J Mass Spectrom 39(12):1441–1449. https://doi.org/10.1002/jms.728

Rodríguez L, Cabrera A, Parra E (2013) Egyptian textiles from Late Antiquity and the Early Middle Ages in Spanish museums: results from three interdisciplinary research projects. In: De Moor A, Fluck C, Linsheid P (eds) Drawing the threads together. Textiles and footwear of the 1st millennium AD from Egypt. pp 108–123

Rosenberg E (2008) Characterisation of historical organic dyestuffs by liquid chromatography–mass spectrometry. Anal Bioanal Chem 391(1):33–57. https://doi.org/10.1007/s00216-008-1977-0

Santos R, Hallett J, Oliveira MC, Sousa MM, Sarraguça J, Simmonds MSJ, Nesbitt M (2015) HPLC-DAD-MS analysis of colorant and resinous components of lac-dye: a comparison between Kerria and Paratachardina genera. Dyes Pigments 118:129–136. https://doi.org/10.1016/j.dyepig.2015.02.024

Sasaki Y, Sasaki K (2013) Analysis of protoberberines in historical textiles: determining the provenance of East Asian textiles by analysis of phellodendron e-Preservation. Science 10:83–89

Sasaki Y, Sasaki K (2017) Dye analysis of a 17th-century historic Japanese textile: a non-destructive approach. In: Kirby J (ed) The diversity of dyes in history and archaeology. Archetype Publications, London, pp 265–277

Stein A (1912) Ruins of desert Cathay: personal narrative of explorations in Central Asia and westernmost China vol I & II. Macmillan & Co, Ltd, London

Tamburini D, Martin de Fonjaudran C, Verri G, Accorsi G, Acocella A, Zerbetto F, Rava A, Whittaker S, Saunders D, Cather S (2018) New insights into the composition of Indian yellow and its use in a Rajasthani wall painting. Microchem J 137:238–249. https://doi.org/10.1016/j.microc.2017.10.022

Wouters J (1985) High performance liquid chromatography of anthraquinones: analysis of plant and insect extracts and dyed textiles. Stud Conserv 30(3):119–128. https://doi.org/10.2307/1505927

Wouters J, Grzywacz CM, Claro A (2010) Markers for identification of faded safflower (Carthamus tinctorius L.) colorants by HPLC-PDA-MS—ancient Fibres, pigments, paints and cosmetics derived from antique recipes. Stud Conserv 55(3):186–203. https://doi.org/10.1179/sic.2010.55.3.186

Wouters J, Grzywacz CM, Claro A (2011) A comparative investigation of hydrolysis methods to analyze natural organic dyes by HPLC-PDA— nine methods, twelve biological sources, ten dye classes, dyed yarns, pigments and paints. Stud Conserv 56(3):231–249. https://doi.org/10.1179/204705811x13110713013353

Zhang X, Corrigan K, MacLaren B, Leveque M, Laursen R (2007) Characterization of yellow dyes in nineteenth-century Chinese textiles. Stud Conserv 52(3):211–220. https://doi.org/10.1179/sic.2007.52.3.211

Zhang X, Good I, Laursen R (2008) Characterization of dyestuffs in ancient textiles from Xinjiang. J Archaeol Sci 35(4):1095–1103. https://doi.org/10.1016/j.jas.2007.08.001

Zhang X, Laursen R, Osipova S (2017) Analysis of dyes in some 19th-century Uzbek suzanis. In: Kirby J (ed) The diversity of dyes in history and archaeology. Archetype Publications, London, pp 339–348